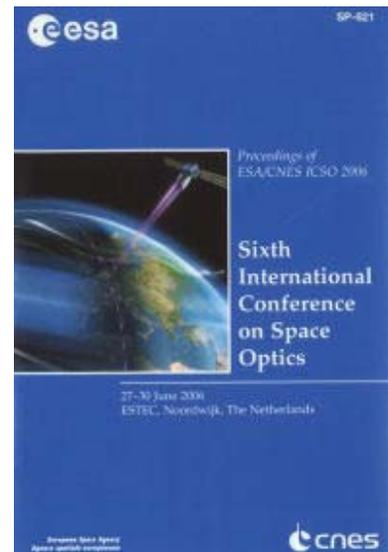# International Conference on Space Optics—ICSO 2006

Noordwijk, Netherlands

27–30 June 2006

Edited by Errico Armandillo, Josiane Costeraste, and Nikos Karafolas

Performance demonstration of a single-frequency optically-pumped cesium beam frequency standard for space applications

S. Lecomte, M. Haldimann, R. Ruffieux, P. Thomann, et al.

PERFORMANCE DEMONSTRATION OF A SINGLE-FREQUENCY OPTICALLY-PUMPED CESIUM BEAM FREQUENCY STANDARD FOR SPACE APPLICATIONS

S. Lecomte, M. Haldimann, R. Ruffieux, P. Thomann, P. Berthoud

Observatoire cantonal de Neuchâtel, Rue de l'Observatoire 58, CH-2000 Neuchâtel, Switzerland
Email: steve.lecomte@ne.ch

ABSTRACT

Observatoire de Neuchâtel (ON) is developing a compact optically-pumped cesium beam frequency standard in the frame of an ESA-ARTES 5 project. The simplest optical scheme, which is based on a single optical frequency for both preparation and detection processes of atoms, has been chosen to fulfill reliability constraints of space applications. With our laboratory demonstrator operated at 852 nm (D_2 line), we have measured a frequency stability of $\sigma_y=2.74 \times 10^{-12} \, \tau^{-1/2}$, which is compliant with the Galileo requirement. The atomic resonator is fully compliant to be operated with a single diode laser at 894 nm (D_1 line). Sensitivity measurements of the clock signal to the microwave power and to the optical pumping power are also presented. Present performance limitations are discussed and further improvements are proposed in order to reach our ultimate frequency stability goal of $\sigma_y=1 \times 10^{-12} \, \tau^{-1/2}$. The clock driving software is also briefly described.

1. INTRODUCTION

Several space applications like navigation systems, telecommunications, long-term missions, and scientific missions require atomic clocks. The system capability is mainly defined by the atomic clock performance. Although atomic clock technology is well mastered for ground systems, they have to be adapted to the space environment in order to exhibit similar performances with rugged packaging and high system reliability as well as with strong reductions of mass, volume and power consumption.

The two atomic clocks foreseen to take place onboard the first generation of Galileo satellites are respectively the Passive Hydrogen Maser (PHM) and the Rubidium Atomic Frequency Standard (RAFS). While the RAFS is a very compact clock (2.4 litres, 3.4 kg), the PHM is bigger (26 litres, 18 kg) [1], but exhibits a 5-fold improvement of the long-term frequency stability σ_y ($< 10^{-14}$ for $\tau > 10^4$ s). These two frequency standards being operated in vapour cell conditions, the influence of the environment is dramatic (frequency temperature coefficient). To overcome the long-term frequency instability of these standards, the atomic-beam frequency standard is an elegant alternative presently in wide use for GPS and GLONASS. Compared to a magnetically-deflected atomic-beam device, a laser-pumped device has a better short-term stability, owing to the fact that it makes use of the full atomic velocity distribution and of the 2-fold increase of the useful atoms due to optical pumping. It can also compete with the PHM in terms of frequency stability. Moreover, due to its inherently simple design, its manufacturing and its reliability can be strongly improved with respect to the PHM.

Observatoire de Neuchâtel (ON) is presently developing such an Optically-pumped Space Cesium Atomic Resonator (OSCAR) in the frame of an ESA-ARTES 5 project. Our goal is to demonstrate a frequency stability of $\sigma_y \leq 1 \times 10^{-12} \, \tau^{-1/2}$ with a compact atomic resonator and only one optical frequency. This choice is motivated by space application prerequisites and has already been discussed [2]. The best measured frequency stability with a 1-frequency scheme is $\sigma_y=4 \times 10^{-12} \, \tau^{-1/2}$ with a compact laboratory atomic resonator and a single laser diode (852 nm, 25-MHz linewidth) [3]. By also using a compact atomic resonator, but a more complex optical setup (2-frequency scheme: one laboratory extended-cavity diode laser and one acousto-optic modulator), the frequency stability was improved to $\sigma_y=1.4 \times 10^{-12} \, \tau^{-1/2}$ using either a Cs beam [4,5] or a Rb beam [6].

In these proceedings, we report on developments of our compact atomic resonator. First we describe the experimental setup (§2), and then we present the experimental results and discuss the current limitations to the frequency stability performances (§3). In §4 the clock controlling software is explained. Finally we present solutions to improve the atomic resonator frequency stability in the conclusion (§5).

2. EXPERIMENTAL SETUP

The architecture of the frequency standard is shown in Fig. 1: the Physics Package (PP) is composed of the Atomic Resonator (AR), while the Opto-Electronics Package (OEP) contains the Optics and Laser modules (OL), the Optics and Laser Control module (OLC) and the Atomic Resonator Control module (ARC).
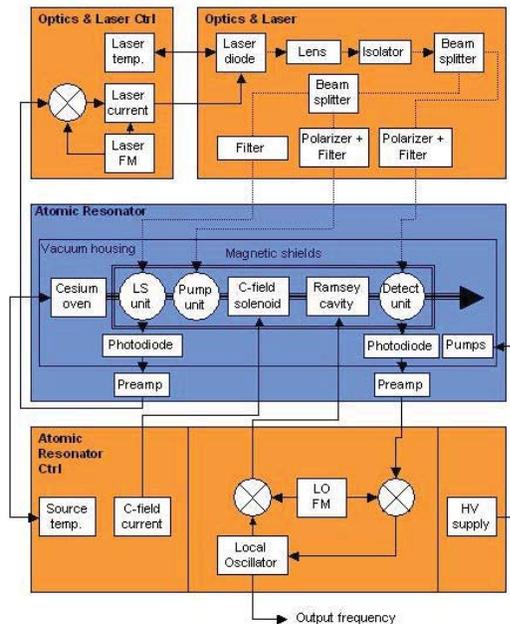

Fig. 1 : Block diagram of the Optically-pumped Space Cesium Atomic Resonator (OSCAR). The blue module in the middle is the Physics Package and the orange side modules are parts of the Opto-Electronics Package.

The AR is fairly standard for an optically-pumped atomic beam resonator. An oven containing Cesium, fitted with a multi-channel collimator, produces the atomic beam. The atoms cross a first laser beam in the Laser Stabilization Unit (LSU), which takes advantage of the fluorescence signal to stabilize the laser frequency. Then, the atoms propagate through a second zone to achieve the required ground state population inversion (Pumping Unit, PU). Subsequently, the atomic beam crosses a short Ramsey cavity (12 cm), where the microwave resonance takes place. Finally, the atomic beam crosses the third laser beam (generated by the same laser) in the Detection Unit (DU), in which the final atomic state is optically probed. In both the LSU and in the DU, the atomic beam fluorescence light is first collected by a specially-machined optical reflector, then converted into photo-current by a Si photodiode placed under vacuum, and finally converted into a photo-voltage by a low noise pre-amplifier outside of the vacuum enclosure. The

three optical units and the microwave cavity are surrounded by a solenoid coil, which produces a uniform magnetic C-field. The AR is maintained under ultra high vacuum by Cesium getters (graphite) and by a commercial ion pump.

The OL has been assembled to operate the atomic resonator with the 1-frequency scheme. Note however that it could be easily adapted for the 2-frequency scheme, by simply adding an acousto-optic modulator to frequency shift the laser detection beam. The optical beam propagates in free space. The single 852-nm laser source is a Distributed Feed-Back diode (DFB), with an output power > 15 mW and a spectral linewidth < 2 MHz. The diverging laser beam is first collimated, then isolated (40 dB), and finally split into three beams. Neutral density filters and polarizers properly prepare their respective power and polarization before entering the AR by windows.

The ARC is composed of the necessary power supplies and driving electronics for the Cs oven temperature regulation, for the C-field solenoid current provision and for the ion pump high voltage supply. The microwave frequency chain (local oscillator, frequency multiplier and phase modulator) is a commercial device. The frequency locking of the quartz oscillator and of the laser diode are performed digitally in a single Digital Signal Processor (DSP). In addition, the C-field amplitude and the RF interrogation power servo-loops are implemented sequentially with the quartz frequency servo loop (see §4). Their different relevant parameters such as modulation amplitudes, gains, duty cycle and filter topologies can be adapted very conveniently with a digital electronics. Moreover it offers additional capabilities such as automatic atomic line searching, which however has not yet been implemented.

The OLC uses the Cesium beam inside the AR as the frequency discriminator (LSU photo-detector). The laser frequency is modulated by its injection current at 10 kHz and locked on the pumping transition line Cs D2:44' by synchronous detection. This hyperfine transition has been chosen for its highest population inversion ratio (15.5%), and for its high fluorescence yield (2.4 ph/at) [7]. Because of the residual cesium vapor in the LSU, the frequency of the fluorescence peak, which is on the side of a broad Doppler background, has a frequency offset with respect to the same hyperfine transition peak in DU (no residual Cs vapor, so no Doppler background). This offset is electronically corrected in order to minimize the clock signal noise.

3. EXPERIMENTAL RESULTS

3.1 Optical parameters

The two fluorescence light collection optics with 100-mm^2 silicon photodiodes collect about 24% of the fluorescence photons. Ideally the collection efficiency should be 42%. This is justified by the fact that the quantum selection rules of the Cs D2:44' transition emits 2.4 photons on average until the atom has changed its quantum state and becomes optically transparent to the laser light. This implies that there is optimum collection efficiency at $1/2.4 = 42\%$: lower detection efficiency will reduce the available Ramsey signal whereas higher detection efficiency will introduce additional partition noise. This collection efficiency is presently limited by the optical surface quality, and by the low reflectivity of aluminum at 852 nm.

Birefringent optical elements create a transverse polarization gradient of the laser beams in the PU and the DU. As these laser beams cross the atomic beam perpendicularly, atoms are always subjected to longitudinal polarization gradient along their path through the laser beams (patent pending, [8]). Such a polarization gradient along the atomic beam increases the efficiency of the optical pumping in the PU without requiring a strong static magnetic field [9], or a 1D optical molasses [10].

The optical power in both the PU and DU was optimized for maximizing the SNR in order to increase the frequency stability of the standard. In the PU, the atoms are optically pumped with 1 mW of optical power whereas they are optically detected with 150 µW in the DU. In the LSU, the SNR for laser stabilization is maximum with 35 µW of optical power.

3.2 Ramsey signal, stability and noise budget of the clock

In Fig. 2, the central Ramsey fringe recorded at an oven temperature of 130 °C is plotted. The corresponding useful atomic flux (atoms in the $m_F = 0$ hyperfine state) has been measured with an ionization detector and reached 4.2×10^9 at/s. A weak and uniform C-field of 52 mG is applied over all optical units (LSU, PU, and DU) and over the microwave Ramsey cavity (Fig. 1). The RF power is adjusted for maximizing the clock signal. The AR has the following performances: the atomic linewidth is 940 Hz, yielding an atomic quality factor of 10^7, the Ramsey central fringe peak-to-valley photo-current is 727 pA, the background photo-current is 1.1 nA, and the noise current density

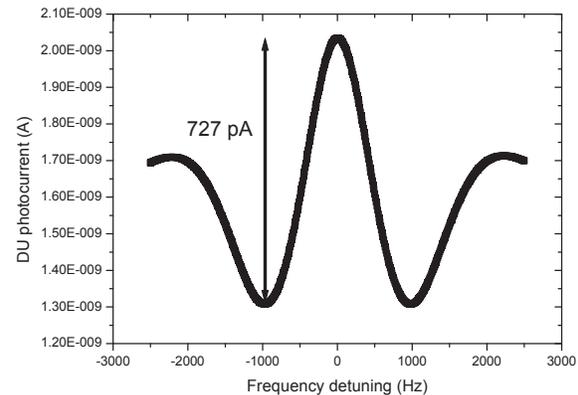at resonance is of 49 fA/Hz$^{1/2}$ yielding a clock SNR of 14'800 Hz$^{1/2}$.

Fig. 2: Ramsey central fringe recorded with an oven temperature of 130 °C.

By operating the atomic resonator with these optimal parameters, and frequency locking the quartz local oscillator with the digital electronics, we have measured its frequency stability with respect to an active hydrogen maser (Fig. 3). The Allan standard deviation extrapolated down to 1 s gives at short-term frequency stability of $\sigma_y = 2.74 \times 10^{-12} \, \tau^{-1/2}$. To the best of our knowledge, this frequency stability is the best ever measured with a compact optically-pumped atomic beam frequency standard operated with a single optical frequency scheme (single laser diode, but no acousto-optic modulator). For short integration time constants (up to 10 s), the improved short-term frequency stability with respect to the atomic resonator performance extrapolation is due to a better quartz frequency stability coupled with a short time constant of the quartz frequency lock loop. For long integration time constants (from 2000 s), environmental magnetic and thermal perturbations degrade the clock frequency stability. For this laboratory demonstration, we remind that only a single magnetic shield is assembled. Moreover, neither C-field nor RF power servo loops are operating here (see §4).

Slightly degraded frequency stability performances ($\sigma_y = 8.5 \times 10^{-12} \, \tau^{-1/2}$) have been recorded by operating the atomic resonator with a single-frequency scheme at 894 nm [11]. However, the major limiting factor was not identified to be the laser wavelength, but rather the lower available atomic flux. With the present operating conditions of the atomic resonator, similar frequency stability performances are expected.
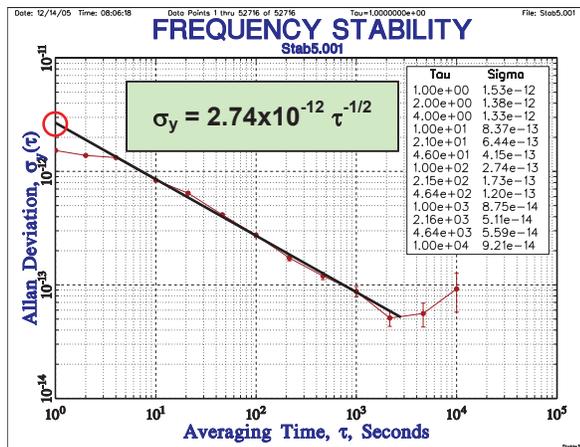
Fig. 3: Measured frequency stability of OSCAR
operated with a single wavelength (852 nm).

Although the stability of the clock is better than the requirement for the Galileo satellite navigation system ($\sigma_y \leq 3x10^{-12} \tau^{-1/2}$), the ultimate frequency stability goal of $\sigma_y \leq 1x10^{-12} \tau^{-1/2}$ has not been yet reached. In fact, the clock noise is not limited by the atomic shot-noise. In the following we will analyze the various noise contributions to the total clock noise and discuss the improvements to be performed in order to increase the clock SNR and reach the atomic shot-noise limit.

In Fig. 4, we plot the different noise current densities as a function of the Ramsey peak-valley photocurrent. The corresponding oven temperatures are given for information.
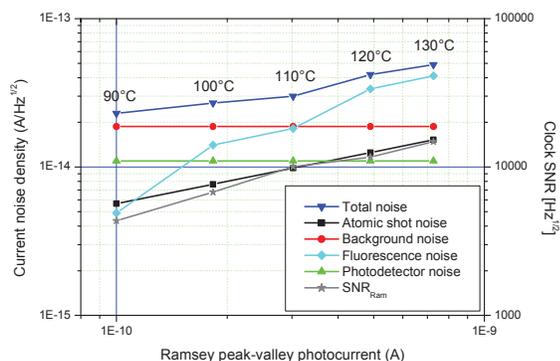

Fig. 4: Noise budget and overall SNR of OSCAR.

We have identified four noise contributions in the clock signal noise budget:

1. Photodetector noise: it is measured in the dark and is independent of the Ramsey photocurrent; for nominal operating atomic flux, this contribution is negligible in the overall noise budget.
2. Stray light noise: it is measured with the nominal optical power but off-resonance, is proportional to the square root of the DC stray light level (shot noise), but is independent of

the Ramsey photocurrent; this technical noise contribution is mainly due to excessive light scattering by the optical windows mounted on the vacuum enclosure.
3. Atomic shot-noise: it is calculated as the square root of the atomic signal; presently this noise contribution is largely dominated by the technical noise.
4. Fluorescence noise: it is computed from the total noise minus the other contributions in RMS values. This noise contribution appears to be proportional to the Ramsey signal and is related to the residual frequency noise of the laser converted into amplitude noise by the atomic beam frequency discriminator.

At high atomic flux where the atomic resonator will finally operate, the major noise contribution is the fluorescence noise (Fig. 4). In order to reduce it, the residual frequency noise of the laser has to be minimized in closed loop operation. Presently, our laser stabilization electronics has a very narrow servo-loop bandwidth (<100 Hz), limited by the ADC/DAC stage of our digital electronics. By increasing it by a factor 100, the amount of proportional noise should be reduced to an acceptable value.

The second major noise contribution arises from the stray light level and its associated shot-noise. While the light traps placed under vacuum are sufficiently absorbent, the large amount of stray light is induced by the laser scattering on the optical windows of the vacuum enclosure. New windows of better optical quality with efficient anti-reflection (AR) coating will be mounted and should strongly reduce the amount of stray light. By effectively reducing these two major noise contributions, the total noise of the clock should be close to the atomic shot-noise contribution.

3.3 Clock sensitivity to microwave power and optical pumping power

Preliminary measurements of the clock output signal frequency have been recorded firstly versus the microwave power injected in the Ramsey cavity, and secondly versus the optical power injected in the pumping unit.

The microwave power level that maximizes the Ramsey signal is −3.2 dBm. In order to measure the clock frequency sensitivity versus the microwave power, the injection RF power has been scanned stepwise from −2.71 dBm to −15.5 dBm. The relative frequency difference between OSCAR and an active hydrogen maser is plotted versus the injected microwave power (Fig. 5).
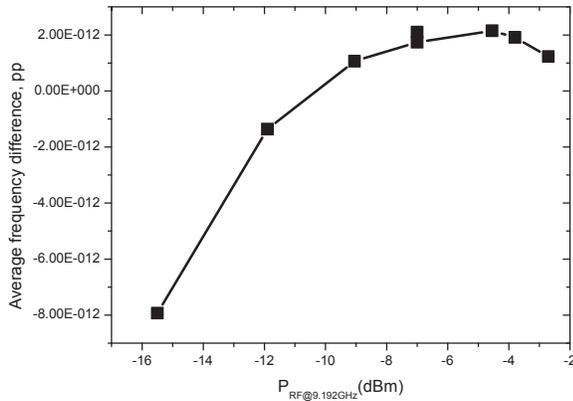
Fig. 5: Relative frequency difference of OSCAR and an active hydrogen maser as function of the injected microwave power.
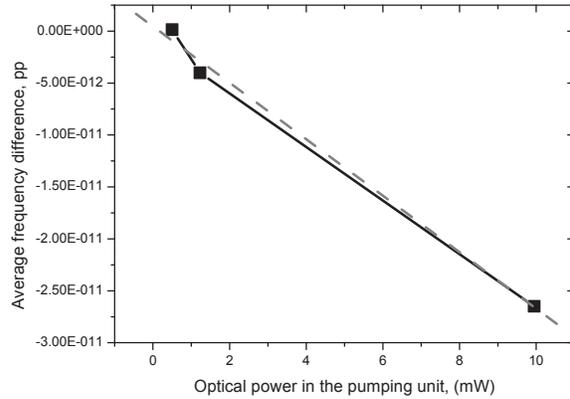

Fig. 6: Relative frequency difference of OSCAR and an active hydrogen maser for different optical pumping powers. The slope of the linear fit is -2.7×10^{-12} mW^{-1}.

Fig. 5 shows that the injection RF power that minimizes the clock output frequency sensitivity (-4.5 dBm of a zero-slope on Fig. 5) is slightly lower than the injection RF power that maximizes the clock signal (-3.2 dBm). Although the short-term frequency stability of the atomic resonator is slightly degraded by operating it at this new injection RF power (lower signal, so lower output SNR), its long-term frequency stability is improved due to minimization of thermal sensitivity of the injection RF electronics chain. This fact has been proven by verifying firstly the longer duration of the $\tau^{-1/2}$ dependence of the Allan standard deviation (up to 10'000 s to reach 4.74×10^{-14}). This averaging duration has to be compared with the Allan standard deviation of Fig. 3 ($\tau^{-1/2}$ dependence only up to 2000 s) in which the atomic resonator was operated at the maximum clock output signal (-3.2 dBm).

The clock output frequency sensitivity to the optical pumping power in the pumping unit has also been investigated. Whereas the optical power that maximizes the SNR is 1.2 mW, the clock output frequency has been measured for 0.5, 1.2, and 9.95 mW (Fig. 6). A frequency variation of -2.7×10^{-12} mW^{-1} has been calculated from the measurements. Compared to previous evaluation of similar developments [12], the light-shift caused by the atomic beam fluorescence should be negligible at a level of 10^{-15}. In this case, the measured light shift should arise of the light scattered in the atomic resonator, which is presently under investigation and improvement.

4. CLOCK DRIVING SOFTWARE

The software architecture of the OSCAR lock loops is shown in Fig. 7. After an initiation phase in which the phase shift is properly adjusted, the quartz oscillator is frequency locked. The periods of the other lock loops (RF power and C magnetic field) can be separately adjusted (parameters T_i with i=1,2,3), as well as the numbers of loops sequences (parameters N_x and M_x), and the loop gains (proportional and integral) via a computer interface.
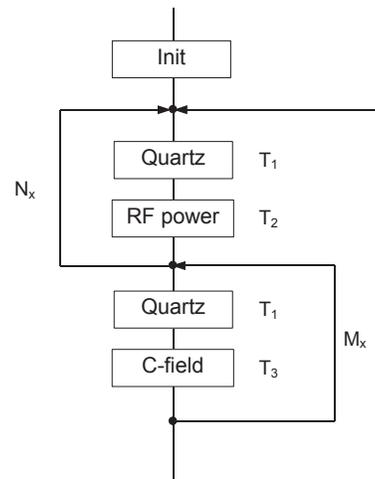

Fig. 7: Software architecture of the OSCAR lock loops.

Presently, we have only tested the capability of the software to lock the C-field whereas opening the lock loop of the quartz. The C-field is measured by interrogating the first Zeeman fringe ($m_F = 1$), and then by feed-backing the control signal onto a stabilized and controllable current source. Preliminary results have

shown that the C-field can be actively stabilized using the atomic beam response without dramatically degrading the output frequency stability. The RF power servo loop has not yet been tested.

5. CONCLUSION and OUTLOOK

We have reported in these proceedings on the experimental setup of an optically-pumped cesium beam frequency standard. Its concept relies on the simplest optical scheme, in which we use only one optical frequency (one laser, no AOM). By depolarizing the laser beams for the optical pumping processes (preparation and detection), we can use a single, uniform and weak magnetic C-field for the optical units without trapping atoms in dark states. A fully digital electronics based on a DSP processor has been specially developed for frequency locking both the laser and the quartz local oscillator. This digital electronics also allows to sequentially lock the magnetic C-field and the RF injection power in the Ramsey cavity. The C-field lock influence on the clock frequency stability has been functionally tested, and no dramatic degradation has been observed due to the loops sequence. The lock of the RF injection power has not yet been investigated. The clock sensibilities to RF injection power and to pumping light shift have also been investigated.

We have demonstrated what is, to the best of our knowledge, the best ever-measured frequency stability of $\sigma_y = 2.74 \times 10^{-12} \, \tau^{-1/2}$ with a compact optically-pumped atomic beam frequency standard operated with a single optical frequency scheme. Although the demonstrated frequency stability is sufficient for Galileo, the clock SNR is not yet limited by the atomic shot-noise. The noise budget has identified the two major noise sources: the "fluorescence noise" and the "stray light noise". While the former could be reduced by increasing the laser frequency servo loop bandwidth, the later will call for top quality optical windows. The marginal fluorescence light collection efficiency will be increased by implementing new and optimize optical collectors. Finally, the presence of a significant Cs vapor pressure close to the oven will be addressed by using more efficient Cs getters. All these improvements are under way in order to reach on OSCAR our ultimate frequency stability goal of $\sigma_y \leq 1 \times 10^{-12} \, \tau^{-1/2}$.

6. ACKNOWLEDGMENTS

7. REFERENCES

[1] F. Droz et al., *The On-board Galileo Clocks: Rubidium Standard and Passive Hydrogen Maser -Current Status and Performance-*, 20th European Time and Frequency Forum, 2006, Braunschweig, Germany, in these proceedings.

[2] P. Berthoud et al., *A feasibility study of an optically-pumped cesium beam resonator for space applications*, 19th European Time and Frequency Forum, 2005, Besançon, France.

[3] P. Petit et al*., Performance of a 2 dm^3 optically pumped cesium beam tube: a progress report*, 8th European Time and Frequency Forum (EFTF), 1994, Munich, Germany.

[4] R. Lutwak et al., *Optically-pumped cesium beam frequency standard for GPS-III*, 33rd Annual Precise Time and Time Interval (PTTI) Meeting, 2001, Long Beach, CA, USA.

[5] S. Guérandel et al., *Compact cesium beam frequency standard: improvements of the frequency stability towards the 10-12 t-1/2 level*, 16th European Time and Frequency Forum, 2002, St-Petersburg, Russia.

[6] A. Besedina et al., *Preliminary results of investigation of the high-stable Rudidium atomic beam frequency standard with laser pumping/detection for space,* 20th European Time and Frequency Forum, 2006, Braunschweig, Germany, in these proceedings.

[7] N. Dimarcq et al., *Comparison of pumping a cesium beam tube with D_1 and D_2 lines,* J. Appl. Phys., 69 (3), p. 1158-1162 (1991).

[8] P. Berthoud and P. Thomann, patent pending.

[9] V. Giordano et al., *New design for a high performance optically pumped cesium beam tube*, IEEE Transactions on Ultrasonics, Ferroelectrics, and Frequency Control, 38 (4), p. 350-357 (1991).

[10] J. H. Shirley and R. E. Drullinger, *Zeeman coherences and dark states in optically pumped cesium frequency standards*, IEEE Prec. Electromagn. Meas., 1994, Boulder, CO, USA.

[11] S.Lecomte et al., *A demonstration experiment of an optically-pumped cesium beam resonator for space*, Proc. of the 1st International Workshop on Optical Clock, 2005, ESA. ESTEC, Noordwijk.

[12] J. H. Shirley, *Fluorescence light shift in optically pumped cesium standards*, Proc. 39th Annual Symp. Freq. Control, 1985, Philadelphia, USA, pp. 22-23